



DEVELOPMENT OF FRAGILITY CURVES FOR THE EVALUATION OF A REINFORCEMENT TECHNIQUE ON URM PATRIMONIAL BUILDINGS IN CARACAS, VENEZUELA

F. Olbrich⁽¹⁾, A. Marinilli⁽²⁾

⁽¹⁾ Universidad Central de Venezuela, olbrich.florian@gmail.com

⁽²⁾ Professor, Instituto de Materiales y Modelos Estructurales. Facultad de Ingeniería. Universidad Central de Venezuela. IMME-FI-UCV, angelo.marinilli@ucv.ve

...

Abstract

The purpose of this paper is to obtain fragility curves to (a) evaluate the seismic vulnerability of a Unreinforced Masonry (URM) patrimonial building in Caracas and (b) the effect of a rehabilitation technique in reducing the seismic vulnerability of the building. The two-story building selected is known as “Casa Amarilla Antonio José de Sucre” and is located in downtown Caracas. This building suffered slight damages during the 1812 earthquake. The strengthening technique studied in this paper consisted of an application of welded steel meshes covered with shotcrete on the URM walls. The log-normal fragility curves were obtained considering four performance levels such as slight, moderate, severe, and complete structural damage. The building, with and without reinforcement, was modelled using the finite element method. Then, several pushover nonlinear analyses were performed to obtain the fragility curves for main orthogonal directions of the building's floor plan. Finally, a study of the rehabilitation technique was performed considering several amounts of steel reinforcement to evaluate the effect of the seismic vulnerability reduction. The results show that vertical and horizontal steel amounts of about 0.62 cm² per meter in each face of the URM walls are enough to achieve seismic vulnerability reductions between 7.5 % and 14.6 % for several earthquake scenarios.

Keywords: Unreinforced Masonry; Fragility Curves; Seismic rehabilitation; Patrimonial Building.

1. Introduction

According to the information provided by the “*Instituto del Patrimonio Cultural de Venezuela*” – IPC [1], in the downtown area of Caracas (AMC), approximately 1.311 patrimonial buildings have been identified (Fig. 1). A significant amount of these structures was built before the 20th Century, implementing an URM System, using Adobe, “*Tapia*” or mixed stone-masonry as construction materials. These buildings showed their vulnerability during the earthquakes of 1812 and 1967, both registering magnitudes of 7.1 Mw and 6.4 Mw respectively [2].

As part of the developments in the characterization of Venezuelan seismic hazard, in 2009, the Seismic Microzoning of Caracas City Project [2] was carried out under the supervision of the Venezuelan Foundation for Seismological Research (Funvisis). This project allowed a detailed characterization of the seismic hazard in the Caracas valley, using specific ground and topographic parameters (Fig. 1).

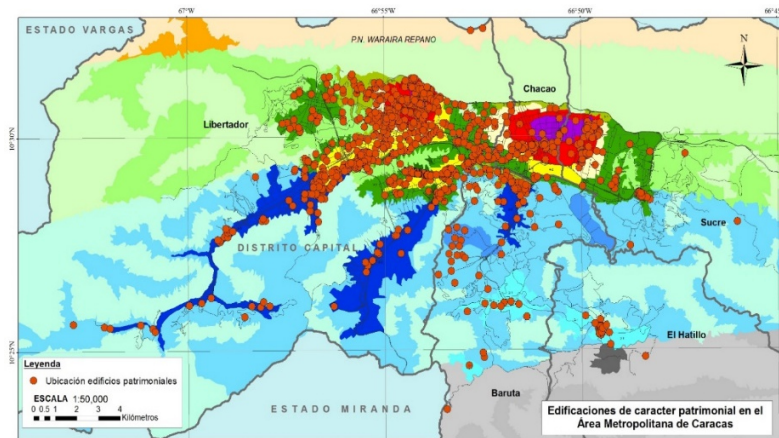


Fig. 1. Location of some Patrimonial Buildings of the AMC in the Microzoning Plane of Caracas [1].

The main purpose of this research is to evaluate the seismic vulnerability of a Unreinforced Masonry (URM) patrimonial building in Caracas, Venezuela. The reasons to execute this research are the need to preserve patrimonial buildings and monuments, which represent a fundamental part of the Venezuelan heritage, the viability offered by recent groundbreaking developments in seismic microzoning and the significant damage caused by past earthquakes. Analytical fragility curves using numerical models were obtained to evaluate the seismic vulnerability of the patrimonial building “*Casa Amarilla Antonio José de Sucre*” located in the AMC. Furthermore, to improve the seismic strength of the building, the strengthening technique for the numerical simulations was taken into the calculation. Finally, a comparative analysis was made between the fragility curves obtained from the original and the reinforced models, to quantify the effect of the strengthening technique on the structural response.

2. Numerical models

The numerical models were developed using the software SAP2000 V15.1.0 [3], which performs nonlinear analysis through the finite element method. The type of element chosen was a shell layered element, because of its capacity to work with different materials while distributing them in several layers with either elastic or inelastic behaviors. The stress-strain curves were defined to represent the direct tension-compression behavior of the material along any of the material’s axes. The shear stress-strain curve was computed internally from the linear stress-strain curve. Although the masonry’s nature is recognized as an anisotropic, the software only allowed simulating orthotropic materials.

The numerical analysis was performed assuming the following mechanical properties: masonry compressive strength (f_m), masonry tensile strength (f_t) and masonry elasticity modulus (E_m), typically determined perpendicular to the bed joints. The elasticity modulus parallel to the bed joints was obtained assuming a value between $0.40E_m$ and $0.5E_m$ [4].

2.1 Casa Amarilla “Antonio José de Sucre”

This structure consists of a URM building built in 1596. It has suffered several interventions since then and it was damaged due to seismic events and fire. Since the beginning of the 20th Century and until now, it was adopted as the seat of The Venezuelan Chancellery. It presents a quadrangular plant with two level of 5.00 m high each one and its primary access leads to the central courtyard. The courtyard is delimited by arcades supported by circular columns. The corridors communicate different meeting rooms and departments of the first and second level (Fig. 2). The ground plan of the building presents an area of 1727.52 m², with 36.6 m width and 47.2 m length.



Fig. 2. Casa Amarilla “Antonio José de Sucre”: Facade (left) and Central courtyard (right).

2.2 Structural and material’s characteristics

The URM walls are made of masonry bricks and in some areas by mixed stone-masonry (Fig. 3). Their thickness varies between a minimum of 50 cm and a maximum of 120 cm. There are 20 masonry circular columns with approximately 25 cm diameter around the courtyard and on both levels (Fig. 2). Concrete slabs reinforced with zen-zen steel meshes form part of the floor and roof system. The slabs rest over steel profiles that are directly supported on the structural walls.



Fig. 3. Structural materials.

The floor and roof system have an approximate rigid diaphragm behavior. Therefore, a diaphragm-constrain was assigned to all nodes contained in the respective planes. In total, 1200 Shell elements related to the URM were defined. Additionally, 40 circular columns were set trough frame elements (Fig. 4). The mean values of the material mechanical properties, as well as their coefficients of variation (COV), have been obtained from bibliographic resources [4], [5] and are defined in the Table 1.

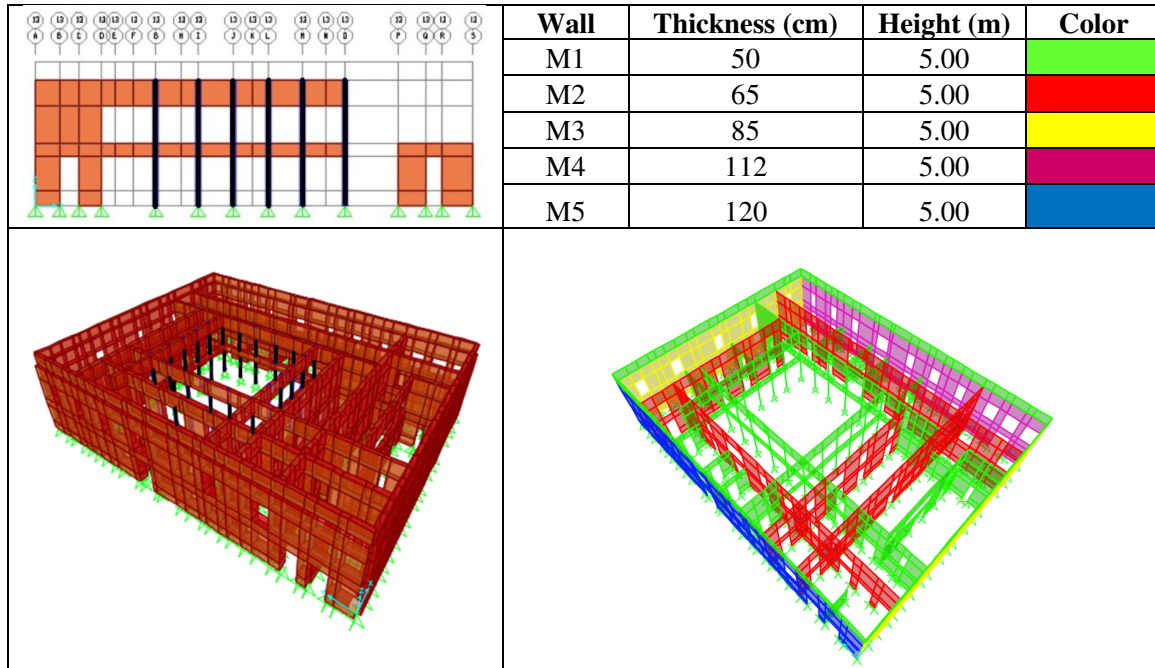


Fig. 4. Characteristics and distribution of the walls in the model.

Table 1 – Mean values and coefficients of variation (COV) of the masonry mechanical properties.

Parameter	Compression Strength f_m (Kgf/cm ²)	Tensile strength f_t (Kgf/cm ²)	Elasticity modulus E_m (Kgf/cm ²)	Poisson ratio μ	Specific gravity γ (Kgf/m ³)	Maximum deformation ϵ_m
Mean	15.00	1.00	10000	0.20	1600	0.005
COV (%)	25	25	30	-	-	45

2.3 Loads

The vertical loads were estimated according to the Venezuelan Building Code COVENIN 2002 [6] and are shown in Table 2:

Table 2 – Vertical loads considered in the simulation.

Level	Permanent loads (Kgf/m ²)	Alive loads (Kgf/m ²)
First Floor	580	500
Roof	500	100

The design spectrum used in the estimation of seismic demands (Fig. 5), was defined according to the Caracas Seismic Microzoning Plan [2]. The building is located in the microzone 4-1 whose characteristics are shown in Table 3. Due to its patrimonial classification, the building belongs to the group A of the Venezuelan building code COVENIN 1756 [7], which attributes it an importance factor $\alpha = 1.30$. For analysis purposes, it was considered a response reduction factor $R = 1.00$ and a critical damping fraction $\zeta = 5\%$. Additionally, to represent the variation

of the seismic demands, it was assumed the variability of the parameter β (spectral mean amplification factor) at 25%.

Table 3 – Response spectrum and soil conditions.

Model	Spectrum	Soil type	Depth of sediments (m)	V _{s30} (m/s)
Casa Amarilla “Antonio J. de Sucre.”	4-1	Sedimentary	60 - 120	>325

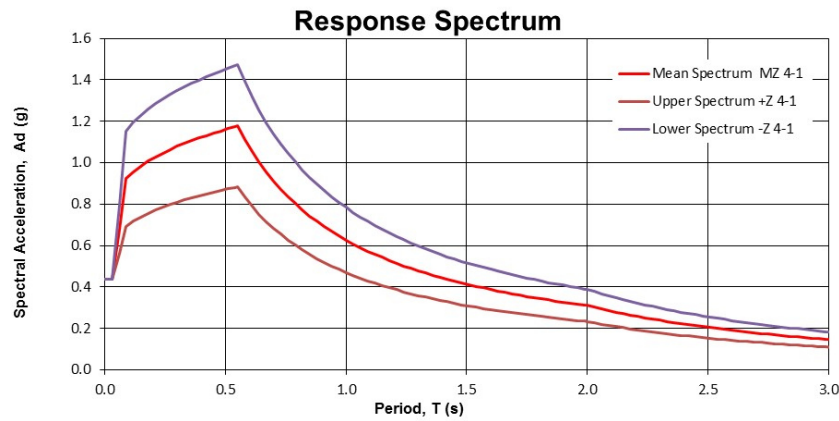


Fig. 5. Response spectrum for microzone 4-1 [2].

3. Capacity curves and probabilistic analysis

The capacity curves, represented as the base shear force versus the deformation on the top of the building, were estimated from pushover analyses according to ASCE/SEI-41 code [8]. The Point Estimate Method was used for the probabilistic analysis [9], which considers that a function of one stochastic variable ($y = f(x)$) can be lumped at two points as showed in Eq. (1):

$$y_+ = f(x_+) = f(m_x + s_x) \tag{1}$$

$$y_- = f(x_-) = f(m_x - s_x)$$

Where m_x is the mean and s_x is the standard deviation of the variable x . The mean and variance of y can be obtained by using the expressions Eq. (2) and Eq. (3) respectively.

$$m_y = y_+ P_+ + y_- P_- \tag{2}$$

$$s_y^2 = (y_+ - m_y)^2 P_+ + (y_- - m_y)^2 P_- \tag{3}$$

Where $P_+ = P_- = P = 1/2$ if the probability function of x is considered symmetrical. This concept can be generalized for functions of several stochastic variables. If the function y involves n stochastic variables, the number of terms will be equal to 2^n and the probability P will be $P = 1/2^n$ assuming that the n variables are independent and have symmetric probabilistic distributions [10].

So, taking the five random variables declared previously, 32 analysis cases in each building’s direction were defined.

The capacity curves in the direction "X" and "Y" (Fig. 6a-b) were obtained after the calibration process of the analysis tool. The reference axes are oriented so that the direction of analysis "X" corresponds to the minor dimension in plant (east- west) and the direction "Y" to the larger plan (north- south).

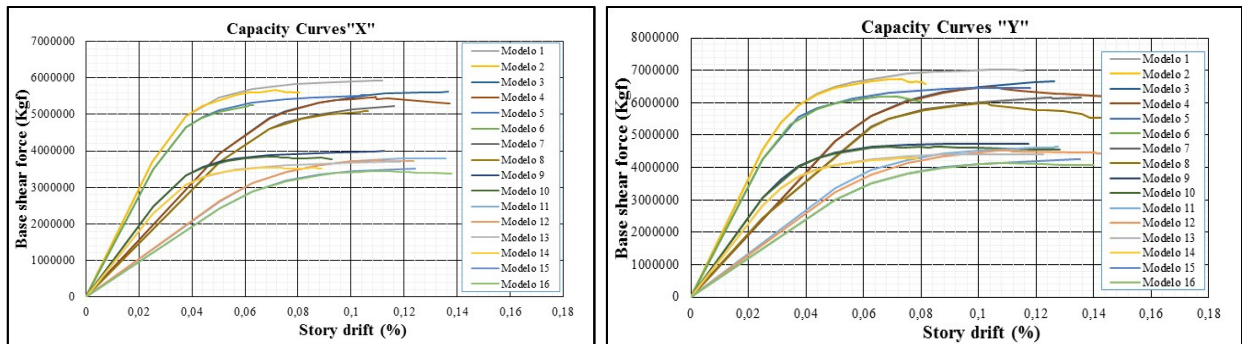


Fig. 6. Capacity curves: **a (left)**: direction “X”; **b (right)**: direction “Y”.

Subsequently, the capacity curves were fitted with three (3) linear segments curve (Fig. 7a), according to the recommendations of the ASCE/SEI-41 code and [11]. The results of the average capacity fitted curves in the two analysis’s direction are presented in Fig. 7b and Table 4. The Maximum strength values exceed 4500 t and 5500 t in direction "X" and "Y", respectively. The initial stiffness in the direction "X" exceeded 8000 t /cm and in "Y" 10000 t/cm.

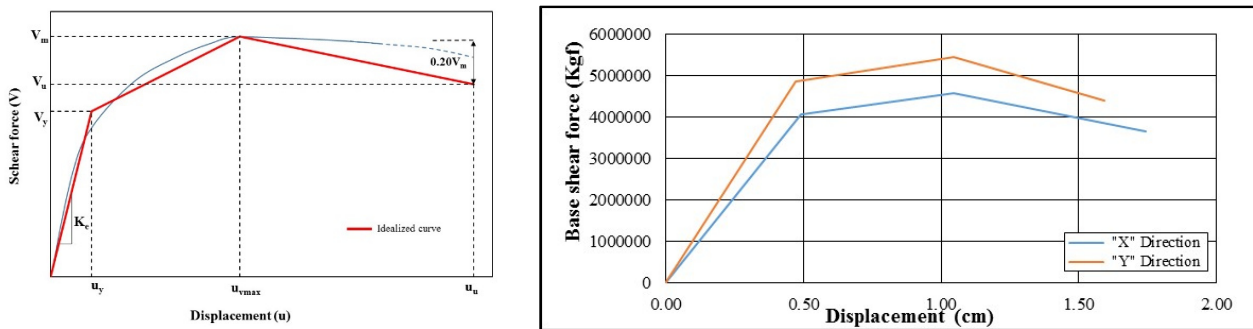


Fig. 7. **a (left)**: trilinear idealization; **b (right)**: average capacity curves.

Table 4 – Displacement limit values and base shear force in both directions of analysis.

Direction	Te (s)	Displacement (cm)			Base shear force (Kgf)		
		Uy	Um	Uu	Vy	Vm	Vu
X	0.134	0.493	1.046	1.744	4060880	4587171	3669737
Y	0.123	0.473	1.047	1.592	4854712	5455997	4408357

4. Fragility curves

4.1 Damage levels

Different authors have proposed deformation limits for URM structures according to the description of damages observed in laboratory tests as well as in seismic performances. Taking the references [12], [13], [14] and the work developed in Venezuela [15], the damage levels indicated in Table 5 were defined.



Table 5 – Description and damage level limits.

d	Damage levels	Description	Displacement
0	No damage	No structural damage. The possible presence of thin cracks in few walls. Drop small pieces of frieze	$< 0.5 u_y$
1	Slight	Cracks in many walls. Drop large chunks of frieze. Partial collapse of chimneys	$u_1 = 0.5 u_y$
2	Moderate	Long and extensive cracks in most walls. Falling tiles. Breaking chimneys in the roofline; failures of some of the non-structural elements.	$u_2 = u_y$
3	Severe	Severe failure of walls; partial structural failures of roofs and floors.	$u_3 = u_y + 0.25 (u_u - u_y)$
4	Complete	Complete or partial collapse.	$u_4 = u_u$

4.2 Displacement demands

The seismic displacement demands (u) were estimated using the Coefficients Method (Eq. (4)) [8].

$$u_d = C_0 C_1 C_2 S_a \frac{T_e^2}{4\pi^2} g \quad (4)$$

Where:

u_d : displacement demand on the upper level of the structure.

S_a : spectral acceleration of the elastic analysis direction equivalent of effective period T_e and damping of 5%

g : gravity acceleration

C_0 : correction factor that correlates the displacement of the upper floor with a system that has one degree of freedom.

C_1 : correction factor that correlates the maximum displacement of the inelastic system with the elastic system.

C_2 : correction factor that represents the throttle effect on the capacity curves against the deformation, stiffness degradation and strength loss of the maximum displacement.

4.3 Fragility curves

The fragility curves provide the probability that the response of the structure reaches or exceeds a threshold associated with a damage level, based on the seismic intensity. The fragility curves were obtained from the curves of capacity and demands, based on the damage levels previously defined. The fragility curves were adjusted using a lognormal distribution [16], determined by Eq. (5).

$$P[D \geq d/A] = \Phi \left[\frac{1}{\beta_{A_d}} \ln \left(\frac{A}{\bar{A}_d} \right) \right] \quad (5)$$

Where:

A : normalized horizontal acceleration of the soil, being the gravity equal to 981 cm/s²

\bar{A}_d : average value associated with the initial damage level

β_{A_d} : standard deviation of the $\ln(A)$ for each damage level

Φ : cumulative distribution function of the standard normal distribution

$P[D \geq d/A]$: The probability of the damage D over the structure conditioned to the occurrence of A

Figure 8a-b represents the fragility curves in "X" and "Y" respectively, as well as the median (A_0) and deviation (β_n) values for both directions.

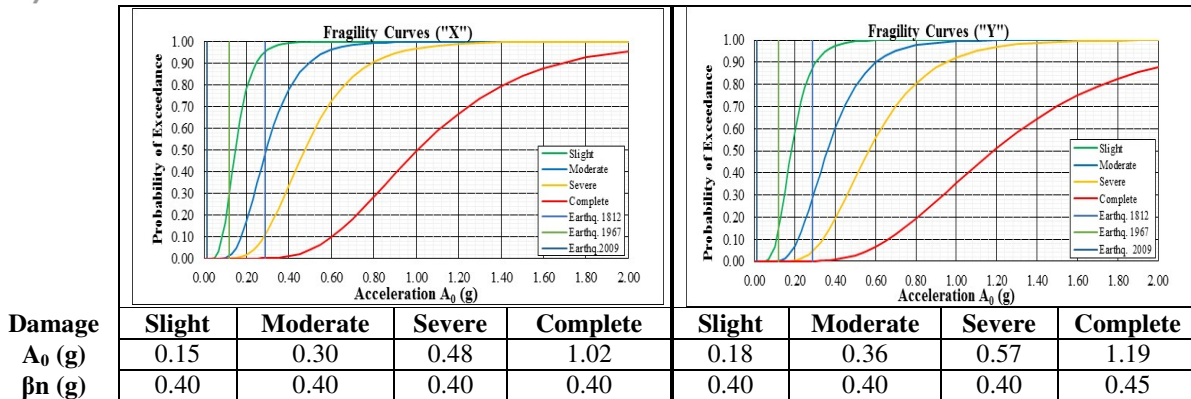


Fig. 8. Fragility curves of building’s actual conditions: a (left): direction “X”; b (right): direction “Y”.

4.4 Validation based on seismic events

A key part of the research consisted of comparing the results of fragility curves with seismic events that had affected the city of Caracas. Thus, Table 7 exhibits the date of the events, their location coordinates, magnitude, estimated acceleration (A_0) and damage reports.

Table 7 – Characteristics of the evaluated seismic events.

Event	Date	Magnitude (Mw)	Latitude	Longitude	A ₀ (g)	Damage
1	26-03-1812	7.5	10.59	-67.33	0,29	Moderate
2	30-07-1967	6.4	10.70	-66.95	0,12	No damage
3	12-09-2009	6.4	10.81	-67.91	0,013	No damage

5. Strengthening strategy

This stage consisted, in the reinforcement of mesh welded wire covered with shotcrete to improve the tensile and shear strength of masonry. A key aspect considered, is that the technique meets the characteristics of compatibility, durability, and reversibility necessary for the intervention of a heritage building, according to the provisions [5]. It is important to note that despite being a technique that generates a great impact on the building; finishing works can ensure the original architecture of the structure. Also, the technic presents the advantage of the availability of materials, skilled laborers, and technology in Venezuela.

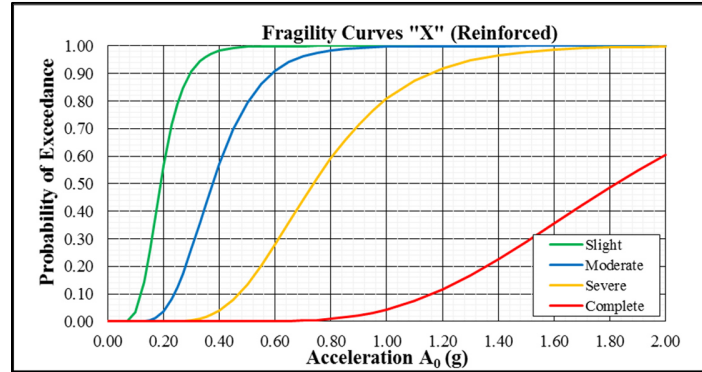
This technique was implemented considering the following characteristics: the reinforcement is applied on both sides of the walls, the layer of shotcrete has a minimum thickness of 3 cm, the meshes have a minimum steel amount of (C1) 0.62 cm²/m, and they are properly anchored horizontally and vertically, including their anchorages at the foundation’s level. The analysis was performed only in the most vulnerable direction of the building (“X”).

Table 8 –Properties of the material of strengthening.

Variable	Nominal value (Kgf/cm ²)	Mean value (Kgf/cm ²)	COV (%)
Compressive concrete strength	f’c = 250	fc = 1.25f’c ; fc = 312.5	15
Steel yield stress	fy = 5000	fy = 1.25fy ; fy = 6250	5

Table 8 contains the mean values and coefficient of variation of the compressive strength of concrete f’c and the steel yield stress fy considered for the strengthening technique. These properties are based on the references [10] and [17]. Likewise, to assess the effect of the variability of these parameters and their influence on the behavior of the building, a sensitivity analysis was performed. This analysis showed that this variability affects only

marginally the capacity curves (less than 6 %). In Fig. 9, the fragility curves in direction "X" of the reinforced model are presented.



Damage	Slight	Moderate	Severe	Complete
A_0 (g)	0.19	0.38	0.74	1.82
β_n (g)	0.35	0.35	0.35	0.35

Fig. 9. Fragility curves of building's reinforced condition (direction "X")

6. Vulnerability curves or damage curves

The vulnerability or damage curves were calculated to compare and verify the results of the evaluation with seismic past scenarios and the influence of the reinforcement strategy on the vulnerability reduction. The vulnerability curves allow us to estimate the average damage on the structure as a function of a seismic intensity (A_0).

The curves are calculated by multiplying the occurrence probabilities of the damage levels, for an intensity seismic level and by a specific damage factors, for masonry structures (Table 9). The vulnerability index is determined by Eq. (6).

$$Iv = \sum_{d=0}^4 \Delta P_d * F_d \tag{6}$$

Where:

Iv : vulnerability or damage index

ΔP_d : the probability of occurrence of damage level "d."

F_d : damage factor

Table 9 – URM building's damage factors.

Damage Level	No damage	Slight	Moderate	Severe	Complete
Damage Factor	F_0	F_1	F_2	F_3	F_4
	0%	25%	50%	75%	100%

Then, five levels of seismic risk were defined: 1) Very Low, 2) Low, 3) Moderate, 4) High and 5) Very High, which are associated with five ranges of vulnerability index (I_v) defined in Table 10, according to [15].

Table 10 – Seismic risk levels.

Seismic Risk Levels					
I_v (%)	< 2.5	2.5 - 10.5	10.5 - 30	30 - 70	> 70
Risk levels	Very low	Low	Moderate	High	Very High

Finally, to study their influence on the reduction of the seismic risk of the building, increments of steel amounts were performed. The comparison between vulnerability curves of the original models and the reinforced models in function of steel amounts are shown in Fig. 10, where $C1 = 0.62$, $C3 = 1.26$ and $C4 = 2.52$, in cm^2/m .

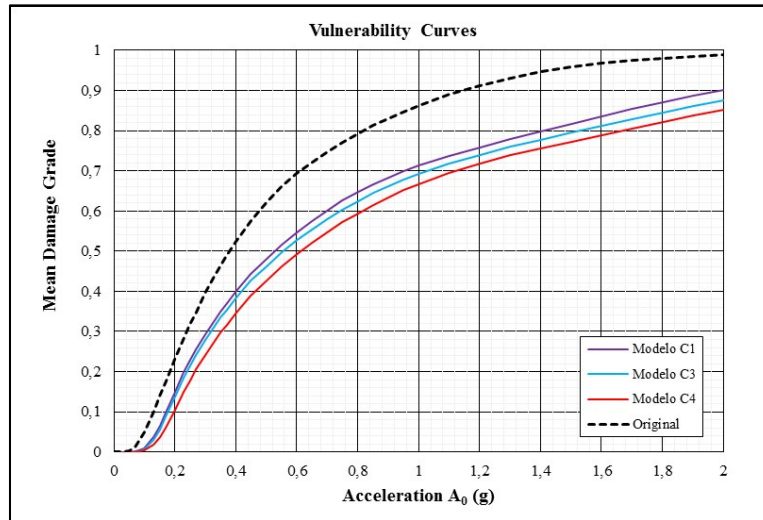


Fig. 10. Vulnerability curves for actual building's conditions and studied steel amounts.

The effect of the strengthening technique and the amount of steel reinforcement was evaluated on three seismic scenarios in Caracas, related to frequent, design, and extraordinary earthquakes (Table 11).

Table 11 –A₀ values for frequent, design and extraordinary seismic events.

Event	A ₀ base value in Caracas (g)	Factor	Return Period (yrs.)	A ₀ (g)
Frequent	0.30	0.50	100	0.150
Design		1.35	1000	0.405
Extraordinary		2.50	10000	0.750

A comparative matrix, based on the resulted vulnerability indexes and risk levels for each seismic scenario is shown in Table 12.

Table 12– Vulnerability indexes and seismic risk levels depending on the amount of steel and seismic scenarios.

Casa Amarilla	Frequent Event	Design Event	Extraordinary Event	Legend
	Vulnerability Index (%)			
Original	14.0%	52.5%	77.1%	Very low
C1	6.5%	39.9%	62.5%	Low
C3	5.7%	38.3%	60.4%	Moderate
C4	3.6%	34.5%	57.2%	High
				Very high

Vulnerability index values in Table 12 show that the reinforcing technique, implemented with any steel amount, reduces the vulnerability index and the seismic risk levels for all seismic scenarios. The maximum reduction is observed comparing original condition and reinforced condition with minimum steel amount (C1). Further increment of steel amount does not show an significant reduction in seismic risk level.

7. Conclusions

The evaluation of the seismic vulnerability of the "Casa Amarilla Antonio José De Sucre" was presented in this paper. The building is an unreinforced masonry patrimonial building located in Caracas, Venezuela. The vulnerability of the building in its current condition was evaluated by means of fragility curves that showed consistency with damages occurred during past earthquakes.



A strengthening technique based on applying welded steel meshes covered with shotcrete was considered to enhance tensile strength of the URM walls. The reinforcing technique is able to reduce the vulnerability index and the seismic risk levels for all the seismic scenarios.

8. Acknowledgments

The authors wish to acknowledge the *Fondo Nacional de Ciencia, Tecnología e Innovación* (FONACIT) for financing the project *SismoCaracas* (No. 2011000716), and the support of the *Fundación Venezolana de Investigaciones Sismológicas* (FUNVISIS), the *Instituto de Materiales y Modelos Estructurales* (IMME), and the *Instituto de Patrimonio Cultural de Venezuela* (IPC) to develop this research.

8. References

- [1] IPC (2004–2007). Catálogo del Patrimonio Cultural Venezolano 2004-2007. Municipio Libertador, Lo Construido. Tomo 2. Ministerio del Poder Popular para la Cultura, Fundación Imprenta de la Cultura, Caracas.
- [2] Funvisis (2009). Informe Técnico Final, Volumen 1 Caracas, Proyecto de Microzonificación Sísmica en la Ciudad de Caracas y Barquisimeto. Caracas: Proyecto FONACIT 200400738.
- [3] CSI (2011). CSI Analysis Reference Manual. Berkeley, California, USA.
- [4] Kaushik, H., Rai, D. C., and Jain, S. K. (2007). Stress-Strain Characteristics of Clay Brick Masonry under Uniaxial Compression. *Journal of Materials in Civil Engineering*: September 2007, Vol. 19, No. 9. American Society of Civil Engineers (ASCE).
- [5] Meli, R. (1998). *Ingeniería Estructural de los Edificios Históricos*. Fundación ICA. A.C., México D.F.
- [6] COVENIN 2002 (1988). Criterios y acciones mínimas para el Proyecto de edificaciones. Comisión Venezolana de Normas Industriales, Caracas.
- [7] COVENIN 1756 (2001). Edificaciones Sismorresistentes. Comisión Venezolana de Normas Industriales, Caracas.
- [8] ASCE/SEI-41 (2013). *Seismic Evaluation and Retrofit of Existing Buildings*. American Society of Civil Engineers and Structural Engineering Institute, Reston, Virginia. USA.
- [9] Rosenblueth, E. (1975). Point estimates for probability moments. *Proc. Nat. Acad. Sci. USA*, Vol. 72, No 10, pp. 3812-3814.
- [10] Marinilli, A. (2009). Análisis probabilístico simplificado de pórticos de concreto reforzado ante acciones sísmicas. *Boletín Técnico IMME*, Agosto 2009, Vol. 38, No. 2, Caracas.
- [11] Tomažević, M. and Lutman, M. (2007). Heritage Masonry Buildings in Urban Settlements and the Requirements of Eurocodes: Experience of Slovenia. *International Journal of Architectural Heritage: Conservation, Analysis, and Restoration*: May 2007, Vol. 1, No. 1, pp. 108-130. Taylor & Francis.
- [12] Calvi, G. M. (1999). A Displacement-Based Approach for Vulnerability Evaluation of Classes of Buildings. *Journal of Earthquake Engineering*: March 1999, Vol. 3, No. 3, pp. 411–438, Taylor & Francis.
- [13] Lagomarsino, S., Penna, A. (2003). Guidelines for the Implementation of the II Level Vulnerability Methodology. WP4: Vulnerability Assessment of Current Buildings. RISK-UE Project: An Advanced Approach to Earthquake Risk Scenarios with Application to different European Towns.
- [14] Barbat A. H., Pujades L.G., Lantada N. and Moreno R. (2008). Seismic Damage Evaluation in Urban Areas Using the Capacity Spectrum Method: Application to Barcelona. *Soil Dynamics and Earthquake Engineering*: October-November 2008, Vol. 28, No. 10-11, pp. 851–865. Elsevier.
- [15] Coronel, G., (2012). Estimación de daños y pérdidas debidas a terremotos en escenarios regionales: aplicación a edificaciones escolares de Venezuela. Tesis de Maestría, Universidad Central de Venezuela – UCV, Caracas.
- [16] McGuire, Robin K. (2004). *Seismic Hazard and Risk Analysis*. MNO-10. Earthquake Engineering Research Institute (EERI). California, USA.
- [17] Porrero, J., Ramos, C., Grases, J., y Velazco, G. (2004). *Manual del Concreto Estructural*. SIDETUR, Caracas.